ADVANCED FUNCTIONAL MATERIALS
www.afm-journal.de

www.MaterialsViews.com

One-Pot Synthesis of Luminescent Polymer-Nanoparticle Composites from Task-Specific Ionic Liquids

*Paul S. Campbell, Chantal Lorbeer, Joanna Cybinska, and Anja-Verena Mudring**

A multifunctional polymerizable ionic liquid, diallyldimethylammonium tetrafluoroborate (DADMA BF_4), is used in a one-pot synthesis of novel luminescent polymer-nanoparticle composites. First, small monodisperse lanthanide fluoride nanoparticles are formed by microwave irradiation in the presence of $Ln(OAc)_3 \cdot xH_2O$ (Ln = Gd, Eu, Tb; OAc = acetate) in the ionic liquid. The nanoparticles can be precipitated for structural characterization or kept in the solution, which yields after irradition by high intensity UV light colorless, processable polymer materials with good photophysical properties. Both green-emitting Tb-containing and red-emitting Eu-containing IL-polymers are described.

1. Introduction

Lanthanide containing materials are becoming more and more essential in our everyday lives. They present strong and distinct luminescent behavior resulting from 4f electronic energy levels, which are little affected by their chemical environments, due to the effective shielding of the f electrons by the filled 5s and 5p external sub-shells. This makes them essential in applications such as energy conversion phosphors for compact fluorescent lamps (CFLs) and LEDs, comprising the energy efficient alternatives to incandescent lamps. In such applications, thin films of luminescent lanthanide materials are used as coatings.[1,2]

One strategy to achieve processable luminescent materials for direct application is through the doping of a flexible matrix with lanthanides. To this end, Ln^{3+}-complexes have been incorporated into organic polymers, liquid crystals and sol–gel derived organic–inorganic hybrids.[3,4] Polymers offer several advantages for the development of materials, such as: flexibility, versatility, optical quality and moderate processing conditions.[5] Indeed, studies involving the doping of polymethylmethacrylate (PMMA) date all the way back to the 1960s, in a study of lanthanide β-diketonates as active components for lasers.[6]

Dr. P. S. Campbell, Dr. C. Lorbeer, Dr. J. Cybinska, Prof. A.-V. Mudring
Anorganische Chemie III–Materials Engineering and Characterization
Ruhr-Universität Bochum
44780 Bochum, Germany
E-mail: anja.mudring@rub.de
Dr. J. Cybinska
Faculty of Chemistry
University of Wrocław
Joliot-Curie 14, 50383 Wrocław, Poland

DOI:10. 1002/adfm.201202472

The incorporation of purely inorganic luminescent materials into polymer matrices has also been investigated.[3,7–11] This presents an even more interesting prospect; combining the advantages of both polymers (good processability and mechanical properties) and inorganic materials (high luminescence efficiency and long-term chemical stability).[3] Fluorides are an important class of inorganic matrix due to their high transparency, wide band gap and low energy phonons, which reduce energy loss through multi-phonon relaxation. Furthermore they are highly chemically stable and physically robust.[12] It is advantageous to synthesize such materials on the nanoscale, with a small and uniform particle size, as this enables us to create ultra-thin homogeneous coatings with high emission intensity while minimizing scattered light. Indeed, particles sized below 40 nm present minimal Rayleigh scattering and transparent materials are obtained.[7] For this reason, in recent years such nanomaterials have been widely investigated.[13] Generally, nanoparticle-polymer composites have been prepared by dispersing the nanoparticles in a solution of a polymer in an organic solvent, followed by preparation of films by spin-coating, dip-coating, or casting.[3] For example, Dekker et al. prepared near-infrared emitting PMMA films doped with LaF_3:Nd^{3+} nanoparticles,[8] while Goubard et al. produced green-emitting Gd_2O_3:Tb^{3+}-doped poly(ethylene oxide) films,[9] and Gipson et al. recently investigated the effect of different capping agents on the synthesis of green-emitting LaF_3:Tb^{3+} doped PMMA.[11]

For the generation of such nanoparticles various methods exist, including hydrothermal,[14] sonochemistry-assisted,[15] microemulsion,[16] microwave-assisted[17] and solution-phase synthesis.[18] Recently, ionic liquids (ILs) already well-established as choice media for nanochemistry,[19] have also been applied to the synthesis of nanoscale lanthanide fluorides.[20] Using microwave techniques has led to promising results with respect to particle size, morphology and photophysical properties.[21] Here, the ionic liquid is used as both the reaction medium and fluoride source (from BF_4^- or PF_6^- anion) as $Ln(AcO)_3 \cdot xH_2O$ is decomposed under MW (microwave) irradiation to give LnF_3 nanoparticles in a controlled manner. A range of different IL cations have been successfully implemented in this process, demonstrating the versatility.

An extensive and ever-growing range of ionic liquids are known.[22] Generally based on organic cations (e.g., ammonium, imidazolium, alkyl phosphonium), facile modifications may be applied such as the addition of functional groups.

Combining this with a wide choice of anions gives us the possibility to design an ionic liquid to a specific purpose or task, hence the commonly coined term task-specific ionic liquids. One such example is the addition of polymerizable moieties. Indeed, much work has been undertaken in recent years in the field of polymerizable ionic liquids (poly-ILs), which have been found to present interesting physico-chemical properties.[23–25] Poly-ILs have a possible application as polymer electrolytes in batteries and fuel cells. They are believed to be a better alternative to many liquid electrolytes, which are flammable, toxic, unstable and prone to leakage.[23,26] To our knowledge, the application of such poly-ILs in the synthesis of luminescent nanoparticles has not been reported. Herein we report a one-pot synthesis of luminescent nanoparticle-polymer composites, from a simple poly-IL, diallyldimethylammonium tetrafluoroborate (DADMA BF_4) using microwave and high-intensity ultraviolet radiation.

2. Results and Discussion

The poly-IL DADMA BF_4 shown in **Scheme 1** was chosen, as BF_4^- acts a good source of F^- upon decomposition, while $DADMA^+$ is a commercially available, inexpensive, and easily polymerizable cation.[24] DADMA BF_4 may be polymerized either by addition of a free radical initiator, for example 1% AIBN (azobisisobutyronitrile), and heating, or by simple irradiation under a high intensity UV-light source. It is known that coloration of ionic liquids is more likely to occur in the presence of impurities and/or when heated due to partial decomposition,[27] therefore the latter polymerization method was favored in our work.

Polymerization of this IL under UV irradiation from a mixture in ethylene glycol results in the precipitation of the polymer as a white powder due to its insolubility. Indeed the polymer is found to be insoluble in most organic solvents and in water, meaning that it can be easily isolated and washed, and has potential for applications exposed to the elements. For processing, the polymer can be cast from a dimethyl sulfoxide (DMSO) solution by slow drying at 100 °C. Alternatively, the powder can be pressed into a transparent film using a hydraulic pellet press.

From the UV-vis absorption spectra of both the monomer IL and the polymer (**Figure 1**) it can be seen that while the ionic liquid monomer is highly transparent in the visible and UV region down to around 220 nm, the polymer film produced is transparent even down to below 200 nm. This can be explained by considering the molecular structure of the polymer compared to that of the monomer, depicted in Scheme 1, as the olefinic bonds responsible for absorption at short wavelengths no longer exist after polymerization. Such highly-transparent polymers show great promise for wide optical application and have the potential for use in phosphor systems excited under UV radiation. Furthermore, thermogravimetric analysis performed on the polymer sample indicates thermal stability up to around 300 °C (Figure S1, Supporting Information). This is good news for potential use in lighting applications, which tend to operate at elevated temperatures (e.g., the working temperature of light-emitting diodes (LEDs) is around 60 °C).

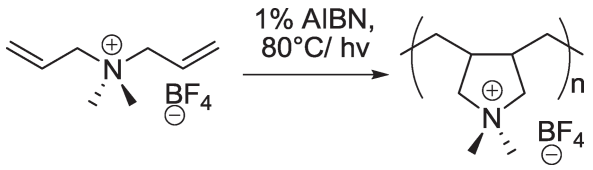

Scheme 1. The polymerization of diallyldimethylammonium tetraßuoroborate.

For the generation of lanthanide fluoride nanoparticles in the polymerizable ionic liquid, our previously developed synthesis procedure was adapted.[21] Firstly, lanthanide acetate hydrates ($Ln(OAc)_3 \cdot xH_2O$, Ln = Gd, Eu, Tb; OAc = acetate) were dissolved in DADMA BF_4. Ethylene glycol (EG), as a co-solvent, is able to facilitate the dissolution process. The solution was then irradiated for 10 minutes using a microwave source (CEM, Discover, USA) operating at 2455 MHz. Following reaction, part of each sample was separated in order to recover by centrifugation and wash (ethanol/CH_2Cl_2) the nanoparticles produced for structural analysis (transmission electron microscopy (TEM), X-ray diffraction (XRD)). The remainder was subsequently irradiated using a high intensity UV lamp (100 W) during a period of 4 h, resulting in a white polymer. This could be washed (ethanol/CH_2Cl_2) and dried to render the product as a powder. The product could be described as poly(diallyldimethylammonium tetrafluoroborate) loaded with 5 wt% LnF_3 as NPs.

In current fluorescent lighting, red and green light are usually achieved by the ions Eu^{3+} and Tb^{3+}, respectively.[1] For this reason polymer-nanoparticle composites were synthesized based on pure EuF_3 and TbF_3 as well as GdF_3 doped with various concentrations of Eu^{3+} and Tb^{3+}; 1, 5, 10 and 20%. GdF_3 acts as a host matrix, diluting the active ions to reduce concentration quenching, with the added advantage of Gd^{3+} efficiently transferring energy to Eu^{3+} and Tb^{3+},[28] and being a promising potential candidate for the conversion of VUV (vacuum UV) radiation.[21,29] Indeed, Eu^{3+} doped GdF_3 has already been reported as a quantum-cutting material, capable of quantum yields greater than unity.[21]

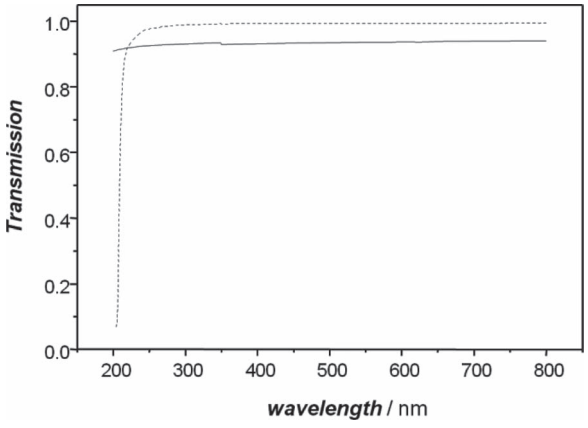

Figure 1. UV-vis transmission spectrum of the ionic liquid monomer DADMA BF_4 (dashed line) and the polymer poly-DADMA BF_4 (solid line).

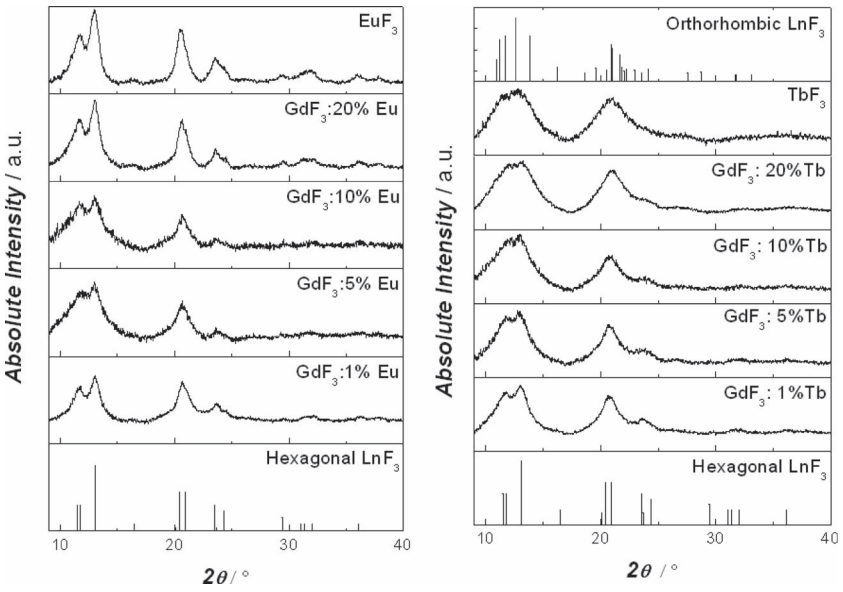

Figure 2. Measured powder XRD diffraction patterns for a) EuF_3 and GdF_3:Eu at various doping concentrations and b) TbF_3 and GdF_3:Tb at various doping concentrations compared to database pattern for hexagonal (JCPDS 32-373) and orthorhombic (JCPDS 12-788) LnF_3.

The measured powder XRD patterns of the isolated EuF_3 and GdF_3:Eu^{3+} particles are shown below in **Figure 2**a, and TbF_3 and GdF_3:Tb^{3+} in Figure 2b. These are compared to the database patterns for LnF_3 both in the tysonite type hexagonal structure (JCPDS 32-373) and in the orthorhombic YF_3-type structure (JCPDS 12-788). It can clearly be seen that all Eu-containing materials adopt the tysonite structure, indicating that under our reaction conditions this is the preferred phase of both EuF_3 and GdF_3, similar to previous results.[21] In contrast, TbF_3 is seen to adopt the lower symmetry orthogonal phase when pure, while GdF_3:Tb adopts the hexagonal phase at low Tb concentration. As the concentration is increased to 20%, a mixture of hexagonal and orthorhombic phase is observed. These results are in accordance with the preference of heavier lanthanides fluorides to adopt the orthorhombic phase.[30]

The broad PXRD peaks can be explained by small crystallite size. To visualize the particle size and morphology, TEM was therefore undertaken on the isolated NPs. Examples of microscopy images obtained for GdF_3:Eu 10% and GdF_3:Tb 10% NPs are shown in **Figure 3**a,b, respectively. More TEM micrographs can be found in the Supporting Information. It can be seen that in each case small nanoparticles are formed with roughly spherical morphologies. Determination of exact particle size of isolated nanoparticle samples is made difficult by the agglomeration of the particles in large aggregates. TEM was therefore also performed on one sample of NPs still contained within the ionic liquid. Here, a drop of NP-IL suspension was deposed onto a carbon film supported on a copper grid, and the excess liquid was removed using filter paper. From images obtained, shown in Figure 3c, individual particles can be more clearly distinguished. This could be explained by the presence of a residual layer of ionic liquid surrounding the NPs and preventing their agglomeration, as already reported in the literature for IL-NP suspensions.[31] From the measurement of over 200 NPs, a size-distribution histogram was constructed, (Figure 3d) showing individual nanoparticle sizes ranging from around 3 to 12 nm with calculated mean diameter of 6 nm ± 2 nm, well below the limit required to reduce light scattering. Small size NPs is not enough to prevent light scattering in a polymer–such nanoparticles must also be well dispersed. Van Veggel's group achieved this feat by the use of stabilizing additives to disperse the NPs in the monomer before polymerization.[13a] In our work the NPs are not to be redispersed in another medium but are to be used in the ionic liquid directly. Therefore, the fact that the ionic liquid inhibits their agglomeration is good news, but does not necessarily ensure the good dispersion in the polymer as phase separation could occur during this process. Example micrographs of the as-prepared nanoparticle polymer composite of GdF_3:Eu 10% are given in Figure 3e, and clearly show that the NPs (darker points) retain their good dispersion within the polymer (dark grey amorphous regions).

Photoluminescence (PL) measurements of all polymer-nanoparticle composite samples were performed at room temperature. Excitation spectra of GdF_3:Eu/Tb at 10% doping concentration are shown in **Figure 4**. Spectra of pure EuF_3 and TbF_3 in the polymer can be found in the Supporting Information. In the case of Eu-containing samples, the emission was monitored at the most intense $^7F_0 \rightarrow {}^5D_1$ transition (590 nm); while for Tb-containing samples the $^5D_4 \rightarrow {}^7F_5$ emission was monitored (541 nm). A series of absorption lines is apparent in each case consistent with the characteristic f–f transitions of Eu^{3+} or Tb^{3+} ions (Figure S4a,S5a, Supporting Information). For Eu^{3+} and Tb^{3+} doped into GdF_3 sharp and more intense bands are also apparent due to $^6I_J \leftarrow {}^8S_{7/2}$ and $^6P_J \leftarrow {}^8S_{7/2}$ transitions characteristic of Gd^{3+}, with maxima at 272 nm, confirming efficient energy transfer from Gd^{3+} to Eu^{3+}/Tb^{3+}. Furthermore, the absence of usually very broad and intense Eu-O charge transfer bands at high UV energies proves that the NPs are oxygen free even in the composite.

Emission spectra were also recorded for all polymer-nanoparticle composite samples. The excitation wavelengths used were 393 nm, 368 nm, and 272 nm for EuF_3, TbF_3 and doped GdF_3 samples, respectively. In **Figure 5** are shown the spectra of GdF_3:Eu (10%) and GdF_3:Tb (10%) nanoparticle-polymer composites (further spectra can be found in the Supporting Information). For Eu^{3+}-containing samples, the intensity of the hypersensitive electric-dipole $^5D_0 \rightarrow {}^7F_2$ transition (610 nm) depends strongly on the site symmetry of the Eu^{3+} ion, whereas the magnetic dipole $^5D_0 \rightarrow {}^7F_1$ transition (590 nm) is insensitive to environmental differences. Calculating the ratio of the intensities of these two transitions gives us the so-called asymmetry ratio, which can be used as an indication of the degree of symmetry of the Eu^{3+} site. Here, this asymmetry ratio is found to vary only slightly from one sample to another, being close to 1 in each case (Figure S8, Supporting Information), in agreement with previous results for Eu^{3+} in the hexagonal-phase fluoride system.[18,21,32]

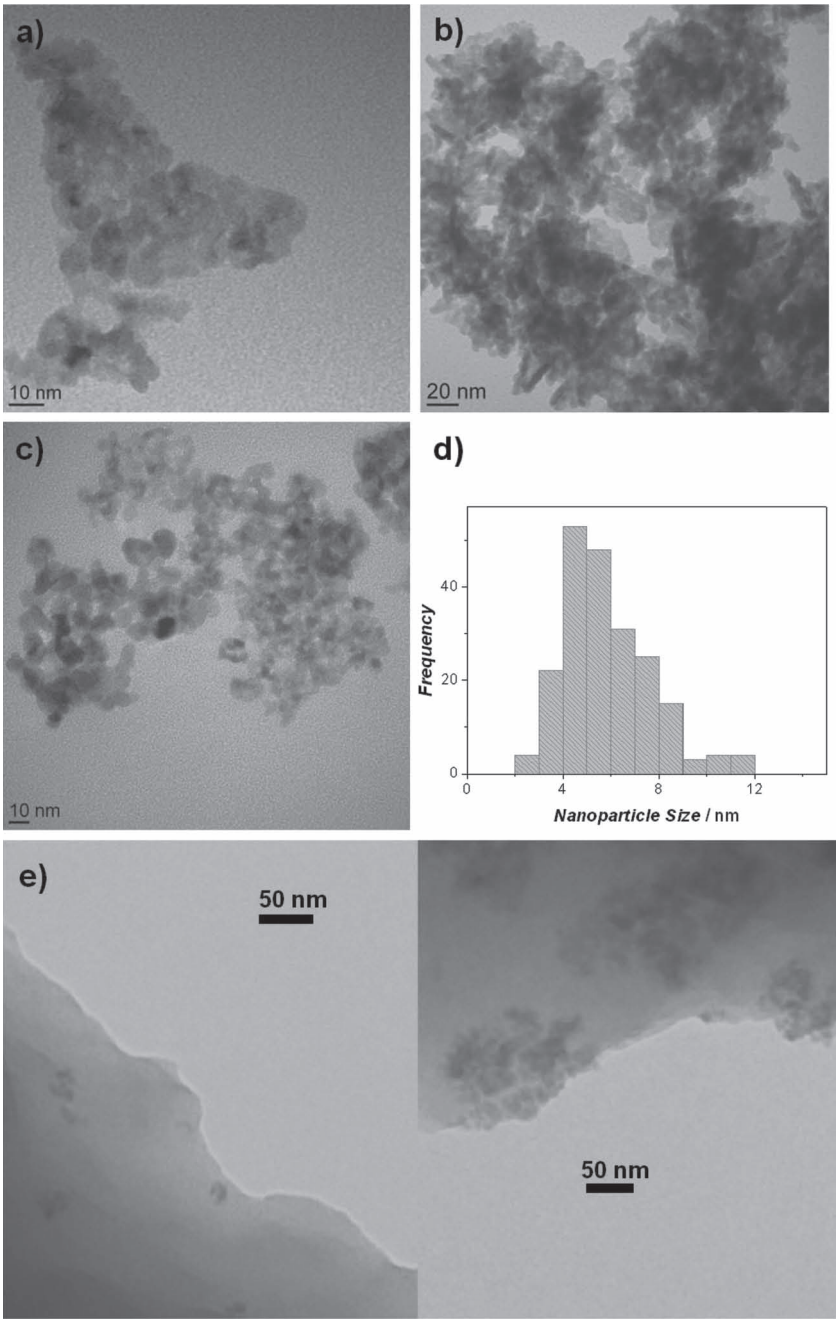

Figure 3. Transition electron micrographs of a) isolated GdF_3:Eu 10%, b) isolated GdF_3:Tb 10% NPs, and c) GdF_3:Eu 10% NPs in the IL DADMA BF_4, with corresponding d) size-distribution histogram, and e) microscopy image of GdF_3:Eu 10% dispersed in the polymer.

In the Eu^{3+} emission spectra, emission from the higher $^5D_1$ level is also observed. This is made possible as the low energy phonons of the GdF_3 host matrix cannot bridge the gap between the $^5D_1$ and $^5D_0$ levels through multiphonon relaxation alone. This is nonetheless quite remarkable, as the presence of high energy oscillators in the organic polymer could be thought to easily quench these emissions. However, as we increase the concentration of the Eu^{3+} in the matrix, this $^5D_1 \rightarrow {}^7F_J$ emission is quickly quenched through cross-relaxation. In **Figure 6** is plotted the intensity ratio between $^5D_1 \rightarrow {}^7F_2$ and $^5D_0 \rightarrow {}^7F_1$ transitions versus the doping concentration of Eu^{3+}. As expected,[33] the intensity ratio decreases with increasing Eu^{3+}, becoming negligible at 20% and non-observable in pure EuF_3 samples (100%).

Unsurprisingly, in both Eu^{3+} and Tb^{3+} systems, emission observed by the naked eye is clearly improved in the doped systems, due to reduction in concentration quenching. This is further emphasized upon measuring emission lifetimes, where for both Eu and Tb samples lifetime increases with decreasing doping concentration, as shown in **Table 1**. Indeed, for pure systems (EuF_3 and TbF_3) the shortest lifetimes are observed. Decreasing lifetimes of optically active ions like Eu^{3+} and Tb^{3+} with increasing concentration is a well-known effect, which cannot be related to the particle's size, nor ascribed to the ions located at the surface. This effect has also been observed for bulk materials or crystals. For Eu^{3+} ions, shortening of the $^5D_0$ lifetime is attributed to the migration-accelerated energy transfer to unintentional traps rather than to the activator–activator interactions.[34] In other words, excitation energy can migrate to traps where it can be quenched non-radiatively. The energy migration and exchange interaction depends on the distance between the optically active luminescent ions, thus is strongly concentration dependent. Furthermore, double-exponentials are needed to fit the decay curves of the pure EuF_3/TbF_3 NP containing samples. This is indicative of ions occupying different sites within the NP, i.e., surface vs. interior, with the shorter component associated to surface ions.[13b] A doping concentration of 100% means a significantly higher proportion of surface activator ions.

In order to better assess the effect of the polymer on the photoluminescence properties, lifetimes of isolated NP samples are also collected in Table 1, all of which are found to be close to those of their polymer composite counterparts. Interestingly, the presence of the polymer seems to bear little detrimental effect on the photophysical properties of the materials, despite the presence of high frequency oscillators, known for quenching luminescence. Indeed, the consistently longer lifetimes measured for the polymer composites could be indicative of a long-term protection provided by the polymer against the adsorption of species such as water or oxygen, whose high energy vibrations would accelerate non-radiative decay.

Photographs of pressed 0.15 mm thick films of the composite samples in daylight and irradiated under 272 nm are given in **Figure 7**, clearly showing the high transparency achieved through small well-dispersed NPs and the

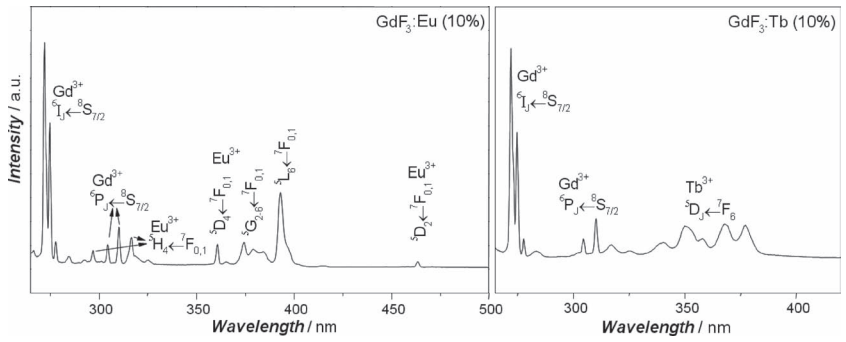

Figure 4. Excitation spectra of GdF_3:Eu 10% (left) and GdF_3:Tb 10% (right) poly-IL-NP composites, emission monitored at 590 nm and 541 nm, respectively.

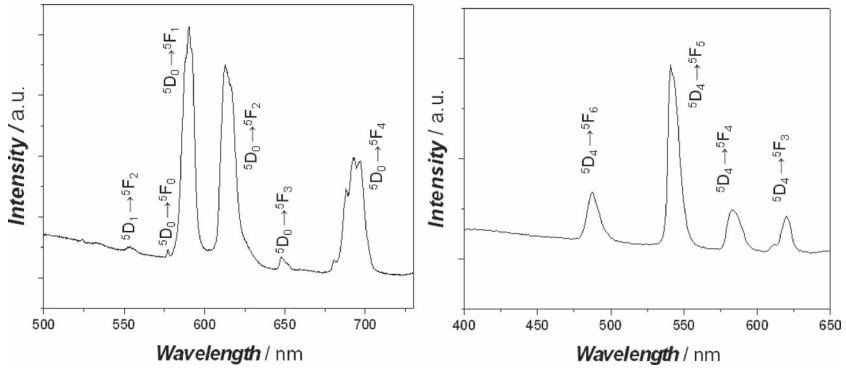

Figure 5. Emission spectra of GdF_3:Eu 10% (left) and GdF3:Tb 10% (right) poly-IL-NP composites excited at 272 nm.

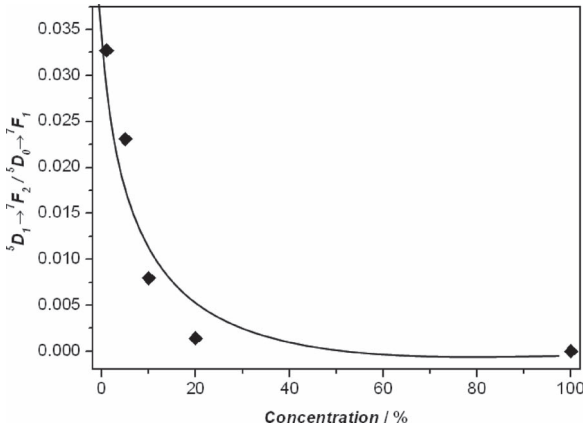

Figure 6. Intensity ratio of $^5D_1 \rightarrow {}^7F_2$ and $^5D_0 \rightarrow {}^7F_1$ transitions plotted as a function of Eu^{3+} concentration in GdF_3.

characteristic red and green luminescence for GdF_3:Eu^{3+} and GdF_3:Tb^{3+}, respectively.

One of the most important parameters allowing us to judge the potential for application of photoluminescent materials is the quantum yield, i.e. number of photons emitted with respect to number absorbed, as this can be directly related to the energy efficiency. The most classical way to determine the quantum yield is through quantitative measurement and comparison of absorbed and emitted light.[35] A white optically-pure reflectance standard must be used, in this case $BaSO_4$, in order to gauge the amount of light absorbed by the sample. Care must be taken in order to ensure that the sample and reference reflect in the same way. Here, this can be achieved by grinding to a fine powder and smoothing to create a flat mirror surface, before running reflectance spectra in an optically inactive region (720 nm). In order to correct for errors due to spectral dependent sensitivity of the lamp and photomultiplier of the photoluminescence spectrometer, a luminescent standard of known quantum yield must also be measured. A popular choice is sodium salicylate, with a quantum yield of 60%, q_{ST}, when excited at a range of wavelengths up to 380 nm. After the required measurements have been performed, Equation (1) can be applied to give corrected quantum yields, q_x, with a 10% margin of error, where r is the measured reflection at the excitation wavelength, and Φ is found by integration of emission spectra.

$$q_X = \left(\frac{1 - r_{ST}}{1 - r_X}\right)\left(\frac{\Delta\phi_X}{\Delta\phi_{ST}}\right) q_{ST} \quad (1)$$

These measurements were carried out on all produced polymer-nanoparticle composites, excited at 368 nm for Tb-containing samples, and at 372 nm for Eu-containing samples. The variation of quantum yield for these samples with respect to concentration of dopant ion Tb^{3+} or Eu^{3+} in GdF_3 is illustrated in **Figure 8**. The negative trend in both cases yet again supports the idea that higher concentrations of activator ion lead to increased concentration quenching. Quantum yields determined in this way varied between 1 and 7%. This appears in line with quantum yields previously determined for simple nanoscale lanthanide doped nanomaterials include SrF_2:Eu^{3+} (QY = 2.5%),[36] and YVO_4:Eu^{3+} (QY = 17–19%).[37]

It is well known that due to the huge surface to volume ratio, the luminescent properties of nanoparticles are strongly

Table 1. Measured emission lifetimes poly-IL-nanoparticle composites and isolated nanoparticles.

Doping Concentration [%]	Lifetime [ms]			
	GdF_3:Eu^{3+}		GdF_3:Tb^{3+}	
	Polymer	NPs	Polymer	NPs
100	0.2, 0.1	0.2, 0.1	0.4, 0.1	0.4, 0.1
20	3.0	2.7	2.0	2.0
10	3.1	2.8	2.7	2.4
5	3.6	3.6	3.4	3.2
1	3.7	3.6	4.3	4.0

GdF_3:Ln samples excited at 272 nm. Emission monitored at 590 nm and 541 nm for Eu^{3+} and Tb^{3+}, respectively. 100% concentration refers to pure EuF_3 and TbF_3 samples, excited at 393 nm and 368 nm, respectively.

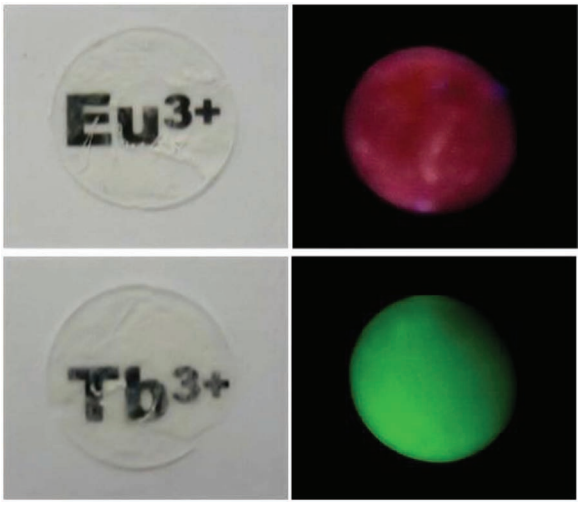

Figure 7. Transparent Þlm of poly-IL-NP composite pellets containing GdF_3:Eu/Tb 10% NPs, viewed in daylight (left) and under 272 nm excitation (right).

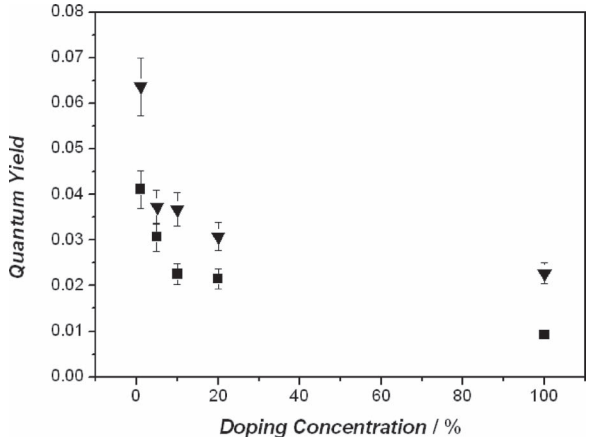

Figure 8. Variation of measured quantum yield of polymer-nanoparticle composite samples with activator ion concentration in GdF_3. GdF_3:Eu@poly-IL (■) excited at 372 nm and GdF_3:Tb@poly-IL (▼) excited at 368 nm.

affected by adsorbed molecules or defects on the surface. Work has been carried out to prevent this quenching including modification of the morphology of the particles or generation of core-shell structures, where the optically active core is coated by wide band gap and optically inactive shell, effectively protecting the activator ions from the quenching processes. As such, high quantum yields have been reported: e.g., $La_{0.4}Ce_{0.45}Tb_{0.15}F_3$/$LaF_3$ core-shell (QY = 42–54%),[13c] $CePO_4$:Tb/$LaPO_4$ core–shell (QY = 70%),[13d] $CePO_4$:Tb/$LaPO_4$ core–shell nanowires (QY = 70%),[13e] $NaYF_4$:20%Yb, 2% Er/$NaYF_4$ upconverting core-shell NPs (QY = 0.18%),[13f] amongst others.

3. Conclusions

In summary, a simple ionic liquid functionalized with polymerizable moieties, namely diallyldimethylammonium tetrafluroborate, has been successfully implemented in a one-pot synthesis for the production of polymer-luminescent lanthanide fluoride nanoparticle composites. This innovative approach exploits the high multi-functionality of the ionic liquid in question as it is used as solvent, stabilizer, fluoride source, and monomer. The principle has been shown to be equally valid for both simple pure lanthanide nanoparticles such as EuF_3 and TbF_3 as well as doped nanoparticles exhibiting superior photophysical properties, e.g., GdF_3:Eu^{3+}, and has potential to be used in conjunction with core-shell particles exhibiting higher quantum efficiency. The polymer produced is transparent, robust; insoluble in water and most organic solvents and thermally stable up to 300 °C (TGA); yet can be processed by casting from a DMSO solution. The presence of the polymer has been shown to have little to no detrimental effect on the subsequent luminescence despite the presence of high frequency oscillators, and could even provide protection against the adsorbtion of nuisance molecules such as water or oxygen on the NP surface. Such novel processable materials could be developed for direct use in various applications, such as energy efficient lighting.

4. Experimental Section

Materials: Diallyldimethylammonium chloride (65% aqueous) was purchased from Sigma Aldrich and the water removed at 80 °C under vacuum prior to use. All other chemicals were purchased from ABCR and used without further puriÞcation.

Ionic Liquid Synthesis: Diallyldimethylammonium chloride (100 g, 0.62 mol) in dichloromethane (200 mL) was added to $NaBF_4$ (68.0 g, 0.62 mol) and stirred at room temperature for 72 h. The Þne white precipitate was removed by Þltration. The clear solution was washed with small quantities of water to remove remaining chloride. The solvent was removed in vacuo and the clear ionic liquid was dried at 80 °C under dynamic vacuum for 24 h. Water level: 36.5 ppm (KarlFischer Titration) 96%. ^{1}H NMR (200 MHz DMSO-d_6, δ): = 6.06 (m, 2H, CH_2-CH = CH_2), 5.63 (m, 4H, CH_2-CH = CH_2), 3.92 (d, 4H, N-CH_2-CH), 2.96 (s, 6H,N$(CH_3)_2$). ^{13}C NMR (200 MHz DMSO-d_6, δ): 49.14, 65.09, 125.74, 127.65.

Nanoparticle Syntheses: $Ln(OAc)_3.xH_2O$ (250 mg) (Ln = Eu, Gd, Tb, Dy) was dissolved in ethylene glycol (2 mL) at 140 °C under rapid stirring. Under argon, this was added to 3 mL of DADMA BF_4 and stirred until homogeneous. 1 mL aliquots of the prepared solution were then transferred to microwave vessels loaded into the microwave (CEM Discover, USA) and irradiated to 100 °C for 10 min with constant stirring. The nanoparticles produced could then be separated by centrifugation, washing with CH_2Cl_2/ethanol, and drying at 70 °C or kept in solution for polymerization.

Polymerization: Nanoparticle containing solutions were irradiated in glass tubes for a period of 4 h using a high intensity (100 W) UV lamp. The solid formed was centrifuged and washed with CH_2Cl_2/ethanol to remove ethylene glycol and unreacted monomer, dried at 70 °C, isolated as a soft white powder. NMR ^{1}H NMR(DMSO-d6): δ = 3.39 (N-CH_2-CH), 3.30 (N$(CH_3)_2$), 3.17 (CH (backbone)). 1.23 (CH_2 (backbone)) (all broad peaks).

Polymer Film Preparation: Transparent polymer Þlms were prepared from 20 mg of as-prepared polymer composite material. This was pressed in a 10 mm die set (MSScientiÞc, Germany) using a MP150 Hydraulic Press (MAASSEN GmbH, Germany), resulting in a transparent Þlm of 150 µm thickness.

Thermogravimetric Analysis: TGA studies were carried out on a TG-50 thermogravimetric analyzer (Shimadzu Corp., Kyoto, Japan) under ßow of dry N_2 gas with a heating rate of 10 K min^{-1}.

Powder X-Ray Diffraction: The powder XRD measurements were carried out on a G670 diffractometer with an image plate detector (Huber, Rimsting, D) operating with Mo Kα radiation.

UV-Visible Absorption Spectroscopy: Visible absorption spectra were measured at room temperature on a Cary 50 spectrometer (Varian, Palo Alto, USA). Liquid samples were loaded into quartz cuvettes (optical special-purpose (OS) glass). Polymer Þlm samples were prepared by dissolving in DMSO and depositing onto a silica slide, followed by drying at 150 °C in a drying cupboard.

Photoluminescence Measurements: Fluorescence and phosphorescence measurements were performed on a Fluorolog FL 3-22 spectrometer (Horiba Jobin Yvon, Unterhachingen, D). A choice between a continuous xenon lamp with 450 W for ßuorescence and a pulsed xenon lamp for phosphorescence measurements is possible. Double gratings for the excitation and emission spectrometer are applied as monochromators. The signal is detected with a photomultiplier. For measurement, powdered samples were Þlled into silica tubes and carefully positioned in the incoming beam in the sample chamber. For quantum yield measurements, ßat powder samples were used, extra care being taken to ensure the sample position for each measurement.

Transition Electron Microscopy: Conventional TEM images were obtained at the Centre Technologique des Microstructures, UniversitŽ Claude Bernard Lyon 1, Villeurbanne, France, using a Philips 120 CX electron microscope with acceleration voltage of 120 kV. To prepare the samples, a suspension of the NPs ethanol was prepared by sonication for 30 min. Subsequently a drop of this suspension was placed onto a carbon Þlm supported by a copper grid and then dried in air. Alternatively, a drop of IL-NP suspension was placed onto a carbon Þlm supported by copper grid and the excess liquid removed using Þlter paper. For observation of the nanoparticle-polymer composites by TEM, the sample was dissolved Þrst in DMSO. A drop was placed onto a copper grid and dried at 100 °C for 24 h. Images were acquired by focusing on the thin edges of the resultant polymer Þlm.

Supporting Information

Supporting Information is available from the Wiley Online Library or from the author.

Acknowledgements

This work was supported by the European Research Council through a starting grant (EMIL contract no. 2008). P.S.C. acknowledges the Alexander von Humboldt Foundation for funding through a Post-Doctoral fellowship. The authors are indebted to Inga Steinunn Helgadottir for TEM measurements and thank undergraduate students Mike Broxtermann and Beth Campbell for their participation on this project.

Received: August 29, 2012
Revised: November 7, 2012
Published online: January 31, 2013

[1] *Practical Applications of Phosphors* (Eds: W. M. Yen, S. Shionoya, H. Yamamoto), CRC Press, Boca Raton **2007**.
[2] *Introduction to Solid-State Lighting* (Eds: A. Zukauskas, M. S. Shur, R. Caska), John Wiley & Sons, New York **2002**.
[3] K. Binnemans, *Chem. Rev.* **2009**, *109*, 4283.
[4] a) L. D. Carlos, R. A. S. Ferreira, V. d. Z. Bermudez, S. J. L. Ribeiro, *Adv. Mater.* **2009**, *21*, 509; b) P. Wang, J.-P. Ma, Y.-B. Dong, R.-Q. Huang, *J. Am. Chem. Soc.* **2007**, *129*, 10620; c) B. Zhao, X.-Y. Chen, P. Cheng, D.-Z. Liao, S.-P. Yan, Z.-H. Jiang, *J. Am. Chem. Soc.* **2004**, *126*, 15394; d) A. Getsis, A.-V. Mudring, *Eur. J. Inorg. Chem.* **2011**, 3217; e) A. Getsis, S.-F. Tang, A.-V. Mudring, *Eur. J. Inorg. Chem.* **2010**, 2172; f) A. Getsis, A.-V. Mudring, *Z. Anorg. Allg. Chem.* **2010**, *639*, 1726; g) A. Getsis, B. Balcke, C. Felser, A.-V. Mudring, *Cryst. Growth Des.* **2009**, *9*, 4429.
[5] J. Kai, M. C. F. C. Felinto, L. A. O. Nunes, O. L. Maltad, H. F. Brito, *J. Mater. Chem.* **2011**, *21*, 3796.
[6] N. E. Wolff, R. Pressley, *J. Appl. Phys. Lett.* **1963**, *2*, 152.
[7] H. Althues, J. Henle, S. Kaskel, *Chem. Soc. Rev.* **2007**, *36*, 1454.
[8] R. Dekker, D. J. W. Klunder, A. Borreman, M. B. J. Diemeer, K. Wšrhoff, A. Driessen, J. W. Stouwdam, F. C. J. M. van Veggel, *Appl. Phys. Lett.* **2004**, *85*, 6104.
[9] F. Goubard, F. Vidal, R. Bazzi, O. Tillement, C. Chevrot, D. TeyssiŽ, *J. Lumin.* **2007**, *126*, 289.
[10] a) J. S. Wang, J. Hu, D. H. Tang, X. H. Liu, Z. Zen, *J. Mater. Chem.* **2007**, *17*, 1597; b) J. C. Boyer, N. J. J. Johnson, F. C. J. M. v. Veggel, *Chem. Mater.* **2009**, *21*, 2010; c) H. Zhang, J. Han, B. Yang, *Adv. Funct. Mater.* **2010**, *20*, 1533; d) E. Tekin, P. J. Smith, S. Hoeppener, A. M. J. van den Berg, A. S. Susha, A. L. Rogach, J. Feldmann, U. S. Schubert, *Adv. Funct. Mater.* **2007**, *17*, 23.
[11] K. Gipson, C. Kucera, D. Stadther, K. Stevens, J. Ballato, P. Brown, *Polymer* **2011**, *3*, 2039.
[12] M. Joubert, Y. Guyot, B. Jacquier, J. Chaminade, A. Garcia, *J. Fluorine Chem.* **2001**, *107*, 235.
[13] a) J. C. Boyer, N. J. J. Johnson, F. C. J. M. van Veggel, *Chem. Mater.* **2009**, *21*, 2010; b) V. Sudarsan, F. C. J. M. van Veggel, R. A. Herring, M. Raudsepp, *J. Mater. Chem.* **2005**, *15*, 1332; c) J. W. Stouwdam, F. C. J. M. van Veggel, *Langmuir* **2004**, *20*, 11763; d) Koempe, H. Bochert, J. Storz, A. Lobo, S. Adam, T. Moeller, M. Haase, *Angew. Chem. Int. Ed.* **2003**, *42*, 5513; e) Y.-P. Fang, A.-W. Xu, W.-F. Dong, *Small* **2005**, *10*; f) A. D. Ostrowski, E. M. Chan, D. J. Gargas, E. M. Katz, G. Han, P. J. Schuck, D. J. Milliron, B. E. Cohen, *ACS Nano* **2012**, *6*, 2686; g) H. SchŠfer, P. Ptacek, H. Eickmeier, M. Haase, *Adv. Funct. Mater.* **2009**, *19*, 3091; h) H. SchŠfer, P. Ptacek, O. Zerzouf, M. Haase, *Adv. Funct. Mater.* **2008**, *18*, 2913.
[14] X. Wang, J. Zhuang, Q. Peng, Y. Li, *Inorg. Chem.* **2006**, *45*, 6661.
[15] R. Yan, Y. Li, *Adv. Funct. Mater.* **2005**, *15*, 763.
[16] J.-L. Lemyre, A. M. Ritcey, *Chem. Mater.* **2005**, *17*, 3040.
[17] Y.-f. Kong, F. Gao, R. He, J. Chen, X. Xu, N. Li, D.-x. Cui, *Curr. Nanosci.* **2010**, *6*, 446.
[18] M. Wang, Q.-L. Huang, J.-M. Hong, X.-T. Chen, Z.-L. Xue, *Cryst. Growth Des.* **2006**, *6*, 1973.
[19] a) M. Antonietti, D. Kuang, B. Smarsly, Y. Zhou, *Angew. Chem. Int. Ed.* **2004**, *43*, 4988; b) E. R. Cooper, C. D. Andrews, P. S. Wheatley, P. B. Webb, P. Wormald, R. E. Morris, *Nature* **2004**, *430*, 1012; c) S. Dai, Y. H. Ju, H. J. Gao, J. S. Lin, S. J. Pennycook, C. E. Barnes, *Chem. Commun.* **2000**, 243; d) J. Dupont, J. D. Scholten, *Chem. Soc. Rev.* **2010**, *39*, 1780; e) J. Dupont, G. S. Fonseca, A. P. Umpierre, P. F. P. Fichtner, S. R. Teixeira, *J. Am. Chem. Soc.* **2002**, *124*, 4228; f) K. Richter, A. Birkner, A.-V. Mudring, *Angew. Chem. Int. Ed.* **2010**, *49*, 2431; g) K. Richter, A. Birkner, A.-V. Mudring, *Phys. Chem. Chem. Phys.* **2011**, *13*, 7136; h) J. M. Pringle, O. Winther-Jensen, C. Lynam, G. G. Wallace, M. Forsyth, D. R. MacFarlane, *Adv. Funct. Mater.* **2008**, *18*, 2031; i) M. He, P. Huang, C. Zhang, H. Hu, C. Bao, G. Gao, R. He, D. Cui, *Adv. Funct. Mater.* **2011**, *21*, 4470.
[20] a) M. He, P. Huang, C. Zhang, F. Chen, C. Wang, J. Ma, R. He, D. Cui, *Chem. Commun.* **2011**, *47*, 9510; b) M. He, P. Huang, C. Zhang, H. Hu, C. Bao, G. Gao, R. He, D. Cui, *Adv. Funct. Mater.* **2011**, *21*, 4470; c) M. He, P. Huang, C. Zhang, J. Ma, R. He, D. Cui, *Chem.–Eur. J.* **2011**, *18*, 5954; d) N. von Prondzinski, J. Cybinska, A.-V. Mudring, *Chem. Commun.* **2010**, *46*, 4393; e) Q. Ju, P. S. Campbell, A. V. Mudring, *J. Mater. Chem. B*, DOI: 10.1039/c2tb00052k.

[21] a) C. Lorbeer, J. Cybinska, A.-V. Mudring, *Cryst. Growth Des.* **2011**, *11*, 1040; b) C. Lorbeer, J. Cybinska, A.-V. Mudring, *Chem. Commun.* **2010**, *46*, 571.

[22] a) *Ionic Liquids in Synthesis (Eds: P. Wasserscheid, T. Welton)* Wiley-VCH, Weinheim **2007**; b) T. Welton, *Chem. Rev.* **1999**, *99*, 2071; c) T. Welton, *Coord. Chem. Rev.* **2004**, *248*, 2459; d) J. P. Hallett, T. Welton, *Chem. Rev.* **2011**, *111*, 3508.

[23] O. Green, S. Grubjesic, S. Lee, M. A. Firestone, *Polym. Rev.* **2009**, *49*, 339.

[24] V. Jovanovski, R. Marcilla, D. Mercerreyes, *Macromol. Rapid Commun.* **2010**, *31*, 1646.

[25] a) H. Ohno, *Macromol. Symp.* **2007**, 551; b) H. Ohno, K. Ito, *Chem. Lett.* **1998**, *27*, 751; c) A.-L. Pont, R. Marcilla, I. De Meatza, H. Grande, D. Mercerreyes, *J. Power Sources* **2009**, *188*, 558; d) M. Yoshizawa, H. Ohno, *Chem. Lett.* **1999**, *29*, 889; e) D. Salas-de la Cruz, A. Mittal, K. I. Winey, R. H. Colby, H. W. Gibson, *Adv. Funct. Mater.* **2011**, *21*, 708; f) S. Lee, G. A. Becht, B. Lee, C. T. Burns, M. A. Firestone, *Adv. Funct. Mater.* **2010**, *20*, 2063.

[26] S. M. Zakeeruddin, M. GrŠtzel, *Adv. Funct. Mater.* **2009**, *19*, 2187.

[27] a) A.-V. Mudring, *Top. Curr. Chem.* **2009**, *290*, 285; b) N. Meine, F. Benedito, R. Rinaldi, *Green Chem.* **2010**, *12*, 1711.

[28] a) Q. Ju, D. Tu, Y. Liu, R. Li, H. Zhu, J. Chen, Z. Chen, M. Huang, X. Chen, *J. Am. Chem. Soc.* **2012**, *134*, 1323; b) P. Ptacek, H. SchŠfer, K. Kšmpe, M. Haase, *Adv. Funct. Mater.* **2007**, *17*, 3834.

[29] E. M. Goldys, K. Drozdowicz-Tomsia, S. Jinjun, D. Dosev, I. M. Kennedy, S. Yatsunenko, M. Godlewski, *J. Am. Chem. Soc.* **2006**, *128*, 14498.

[30] a) A. Zalkin, D. H. Templeton, *J. Am. Chem. Soc.* **1953**, *75*, 2453; b) I. M. Ranieri, S. L. Baldochi, D. Klimm, *J. Solid State Chem.* **2008**, *181*, 1070; c) O. Greis, T. Petzel, *Z. Anorg. Allg. Chem.* **1974**, *403*, 1.

[31] a) L. S. Ott, R. G. Finke, *Coord. Chem. Rev.* **2007**, *251*, 1075; b) H. Bšnnemann, K. S. Nagabhushana, R. M. Richards, in *Nanoparticles and Catalysis* (Ed: D. Astruc), Wiley-VCH, Weinheim **2008**; c) P. S. Campbell, C. C. Santini, D. Bouchu, B. Fenet, K. Philippot, B. Chaudret, A. A. H. Padua, Y. Chauvin, *Phys. Chem. Chem. Phys.* **2010**, *12*, 4217.

[32] M. M. Lezhnina, T. JŸstel, H. KŠtker, D. U. Wiechert, U. H. Kynast, *Adv. Funct. Mater.* **2006**, *16*, 935.

[33] X. Fan, D. Pi, F. Wang, J. Qiu, M. Wang, *IEEE Trans. Nanotechnol.* **2006**, *5*, 123.

[34] P. Solarz, W. Ryba-Romanowski, *J. Phys. Chem. Sol.* **2003**, *64*, 1289.

[35] a) C. d. M. Doneg‡, S. J. L. Ribeiro, R. R. Gon•alves, G. Blasse, *J. Phys. Chem. Solids* **1996**, *57*, 1727; b) M. S. Wrighton, D. S. Gingley, D. L. Morse, *J. Phys. Chem.* **1974**, *78*, 2229.

[36] Y. Jin, W. Qin, J. Zhang, *J. Fluorine Chem.* **2008**, *129*, 515.

[37] A. Zharkouskay, H. LŸnsdorf, C. Feldmann, *J. Mater. Sci.* **2009**, *44*, 3936.